JOURNAL OF APPLIED ELECTROCHEMISTRY 20 (1990) 479–487

Mechanistic and kinetic aspects of silver dissolution in cyanide solutions

J. B. HISKEY

Department of Materials Science and Engineering, University of Arizona, Tucson, Arizona 85721, USA

V. M. SANCHEZ

School of Chemistry, Universidad de Sonora, Hermosillo, Sonora, Mexico

Received 26 June 1989; revised 15 August 1989

The factors influencing the dissolution kinetics of pure silver in cyanide solution have been analysed in terms of an electrochemical mechanism. A kinetic model is presented which incorporates coupled diffusion and charge transfer for the anodic branch, and combined diffusion, adsorption and charge transfer for the cathodic branch. The anodic oxidation of silver has been investigated using a silver rotating-disc electrode for concentrations between 10^{-3} and 10^{-1} M NaCN. Oxygen reduction on silver has been studied at oxygen partial pressures between 0.104 and 1.00 atm. Mechanistic aspects of the oxygen discharge reaction are considered in explaining the kinetic differences between gold and silver dissolution in cyanide solution. It is shown that under conditions typical of conventional cyanidation gold dissolves measurably faster than silver.

1. Introduction

The kinetics and mechanism of gold and silver cyanidation have been the subject of numerous investigations. In fact, some studies predate the cyanide process of MacArthur and Forrest [1, 2]. In spite of this attention, no consensus has been reached regarding the fundamental differences between the rates of gold and silver dissolution in dilute alkaline cyanide solutions.

Some of the early studies on the dissolution of gold and silver in cyanide solutions reveal inconsistent and anomalous kinetic behaviour. In general this early work shows the complex relationship between the kinetic roles of the oxidant and the complexing agent for these metals. As early as 1934, Barsky *et al.* [3] examined the kinetics of the dissolution of pure gold and pure silver in cyanide solutions. They reported the the maximum rates of gold and silver dissolution were 4.58×10^{-9} and 3.42×10^{-9} mol cm^{-2} s^{-1}, respectively, in a 0.01 M NaCN solution at 25° C. They further observed that at dilute NaCN concentrations (0.002 M) the rate of silver dissolution was approximately 3.5-times greater than that of gold dissolution.

The results of Beyers [4] also indicated complex effects between cyanide and oxygen concentrations for gold and silver dissolution. At an oxygen concentration of about 1.72×10^{-4} M the dissolution of both pure gold and pure silver increased with increasing KCN concentration from 1.5×10^{-3} to 3.1×10^{-2} M. At KCN concentrations above 7.7×10^{-3} M the rate of gold dissolution exceeded that of silver. For example, in a 1.54×10^{-2} M KCN solution at 20° C the rates of gold and silver dissolution were 4.69×10^{-9} and 3.10×10^{-9} mol cm^{-2} s^{-1}, respectively. As observed by Barsky *et al.* [3], the rate of silver dissolution was greater than that of gold at dilute cyanide concentrations.

Kakovskii and Kholmanskikh [5, 6] studied the kinetics of gold and silver cyanidation using rotating-disc samples under various conditions. They found that the rate of silver dissolution was measurably faster than that of gold even at high cyanide concentrations. Silver dissolution was 22.2×10^{-9} mol cm^{-2} s^{-1} at 25° C, 7.7×10^{-3} M KCN, 1 atm P_{O_2} and 1100 rpm. By comparison, the rate of gold dissolution under the same conditions was 6.22×10^{-9} mol cm^{-2} s^{-1}. It is interesting to note that at low rotational speeds (150 rpm) gold dissolution rates were higher than those of silver.

Deitz and Halpern [7] examined the kinetics of silver dissolution under various oxygen pressures. At 5.5×10^{-2} M NaCN and 24° C they found that the rate of silver dissolution followed a first-order dependence on the oxygen pressure. At low cyanide concentrations the rate was independent of the oxygen pressure. At 1 atm P_{O_2}, 24° C and 5.5×10^{-2} M the rate of silver dissolution was determined to be 9.66×10^{-9} mol cm^{-2} s^{-1}.

Conventional extraction results reveal that the relative dissolution rate of silver is noticeably lower that that of gold under typical cyanidation conditions. This is illustrated by comparing gold and silver recoveries for several heap leaching operations as shown in Table 1.

These results indicate that the rate of silver dissolution lags behind that of gold in every instance. Naturally, the mineralogy and mode of occurrence play an important role in determining the rate at which each metal is released from the ore. However, the idea persists that silver leaches slower than gold

0021-891X/90 $03.00 + .12

Table 1. Representative gold and silver recoveries from heap leaching (after [28])

Operation	Recovery (%)	
	Au	Ag
Smoky Valley	50	22
Coeur-Rochester	80	50
Zortman-Landusky	65	9
Northumberland	57	20
Borealis	80	25
Tombstone	70	30
Tuscarora	50	40

under similar conditions. To resolve some of the questions a fundamental electrochemical investigation was undertaken to determine the mechanism and rate-determining factors in the cyanidation of silver and to relate them to previous electrochemical studies on the dissolution of gold in cyanide solution [8].

2. Theory

The leaching of metals like gold and silver in cyanide solution is similar to a metal corrosion process. Conventional cyanidation of gold and silver employs O_2 in air as the oxidant and CN^- serves as the complexing agent. Cyanidation proceeds according to the general overall reaction

$$M + xCN^- + \frac{a}{4}O_2 + \frac{a}{2}H_2O = M(CN)_x^{(a-x)} + aOH^- \quad (1)$$

where M represents the metal, and a and x are stoichiometric coefficients. In the case of gold and silver the stable cyano-complexes are the $Au(CN)_2^-$ and $(AgCN)_2^-$ ions, respectively [9].

The leaching mechanism is electrochemical in nature. The anodic dissolution of either gold or silver would proceed according to the reaction

$$Me + 2CN^- = Me(CN)_2^- + e^- \quad (2)$$

where Me is either gold or silver. Wadsworth [10] has analysed the anodic dissolution of gold in terms of coupled diffusion plus surface charge-transfer kinetics. This model provided an excellent explanation of experimental electrochemical (voltage–current) curves measured by Kudryk and Kellogg [8].

The following kinetic treatment involves mixed diffusion plus surface charge transfer. Equation 3 describes the rate of diffusion for CN^- to the metal surface:

$$\left(\frac{dn}{dt}\right)_{CN} = -\frac{AD_{CN}}{\delta}([CN] - [CN]_i) \quad (3)$$

In this equation A represents the electrode surface area, D_{CN} is the diffusion coefficient for CN^-, δ is the boundary layer thickness, and [CN] and $[CN]_i$ are the concentrations of cyanide in the bulk of solution and at the metal–solution interface, respectively. Since the rate of metal dissolution is half the rate of cyanide consumption, Equation 3 can be written to express metal dissolution in terms of cyanide consumption:

$$\left(\frac{dn}{dt}\right)_{Me} = -\frac{1}{2}\left(\frac{dn}{dt}\right)_{CN} \quad (4)$$

The anodic current density (i_a) is related to the rate of metal dissolution by

$$i_a = \frac{z_a F}{A}\left(\frac{dn}{dt}\right)_{Me} \quad (5)$$

where z_a is the total number of electrons involved and F is the Faraday constant. It follows from these expressions that

$$i_a = k_d([CN] - [CN]_i) \quad (6)$$

where $k_d = D_{CN} z_a F/2\delta$.

The relationship used to explain the charge transfer component is the Butler–Volmer equation which shows how the current density (i) across a solid–solution interface depends on the potential. The Butler–Volmer expression for the anodic dissolution of gold or silver in cyanide, neglecting back-reaction kinetics and assuming only one cyanide ion participating in the rate determining step [11], is

$$i_a = k_a [CN]_i \exp\left(\frac{\alpha_a F E_a}{RT}\right) \quad (7)$$

The value of k_a equals $z_a F \vec{k}_a$, where $\vec{k}_a$ is the rate constant for the charge-transfer step. In the exponential term, α_a is the anodic transfer coefficient, E_a is the voltage for the anodic reaction, and other terms have their usual meanings. Assuming steady-state conditions, Equations 6 and 7 may be combined to yield the following expression for the anodic current:

$$i_a = \frac{k_d[CN]}{1 + (k_d/k_a)\exp[-(\alpha_a F E_a/RT)]} \quad (8)$$

As shown by Wadsworth [10], this equation provides an excellent model for the electrochemical data of Kudryk and Kellogg [8] for the anodic dissolution of gold as a function of the KCN concentration.

Now the accompanying cathodic reaction involves the discharge of oxygen at the metal surface. The kinetics and the mechanism of the oxygen reduction reaction on different electrode materials has been investigated extensively [12–22]. Oxygen reduction on a metal surface has been found to follow two reaction pathways: one is the direct $4e^-$ path represented for alkaline solutions by the overall reaction

$$O_2 + 2H_2O + 4e^- = 4OH^- \quad (9)$$

and the other is the $2e^-$ sequential path involving the formation of hydrogen peroxide ions as an intermediate product and the reduction of hydrogen peroxide ion to yield OH^-:

$$O_2 + H_2O + 2e^- = HO_2^- + OH^- \quad (10)$$

$$HO_2^- + H_2O + 2e^- = 3OH^- \quad (11)$$

Both the direct pathway and the sequential pathway

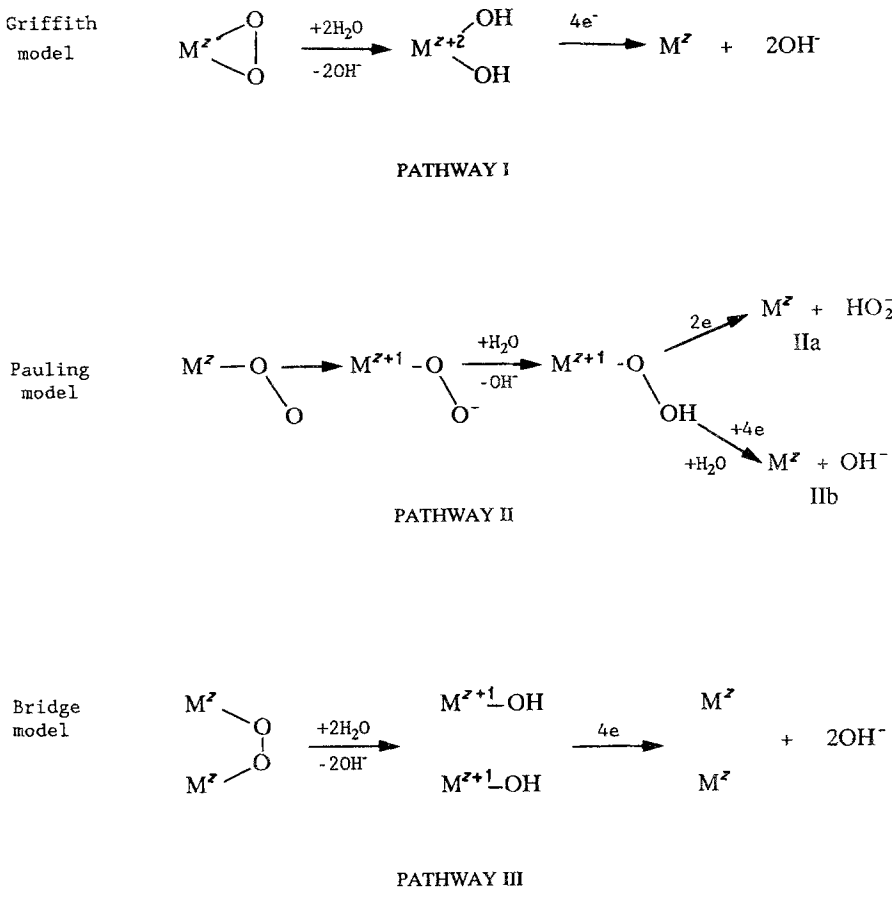

Fig. 1. Models for O_2 adsorption at the electrode surface and subsequent reaction pathways for O_2 reduction in alkaline solution (after [24]).

occur by the initial adsorption of O_2 at the metal surface [13, 14, 17, 19, 23]. Oxygen reduction mechanisms at different electroactive surfaces have been analysed by Yeager [24] for alkaline solutions. Mechanistic models for O_2 adsorption at a metal surface and subsequent O_2 reduction pathways are shown in Fig. 1.

The 'end-on' adsorption model, $M^{\diagup O-O}$, is the only pathway of the three that favours the two-electron reduction of oxygen to HO_2^-. Numerous studies have shown that on gold pathway II predominated [12, 13, 17, 20]. Pathways I and III involve the dissociative adsorption of oxygen, which requires a strong metal–oxygen interaction, sufficiently strong to weaken the O–N bond. There is substantial evidence that dissociative adsorption (that is, four-electron reduction of O_2) predominates on pure Ag substrates [13, 17]. Fischer and Heitbaum [13] concluded from molecular orbital calculations that on pure Ag that the four-electron bridge adsorption pathway is operative and that on gold the two-electron 'end-on' pathway is operative. Furthermore, it was demonstrated that impurities cause the bridge mechanism in silver to shift to the 'end-on' adsorption. Juttner [17] examined the reduction of oxygen on gold and silver in the presence of underpotential-deposited metal atoms of Pb and Bi. On clean Ag substrates the four-electron oxygen reduction takes place according to the $M^{\diagup O-O}\diagdown Me$ model. Whereas the presence of either Pb or Bi blocked neighbouring surface sites necessary for oxygen bridging and forced the reaction into the 'end-on' adsorption pathway. It was further demonstrated that adatoms of Pb and Bi on gold caused a positive catalytic effect, indicating a shift from the 'end-on' to a bridged complex, a bridged complex $Au^{\diagup O-O}\diagdown M'$ (M' = Pb or Bi). It is significant that the fundamental investigation of Juttner [17] serves to explain why the presence of small additions of lead, mercury, bismuth and thallium accelerate the rate of gold dissolution during cyanidation [25]. The general sequence of steps for oxygen reduction is as follows:

$$O_2(b) \xrightarrow{\text{diff}} O_2(i) \tag{12}$$

$$O_2(i) \overset{K}{\rightleftharpoons} O_2^* \tag{13}$$

$$O_2^* \underset{k_{-2}(-2e^-)}{\overset{k_2(+2e^-)}{\rightleftharpoons}} HO_2^- \tag{14}$$

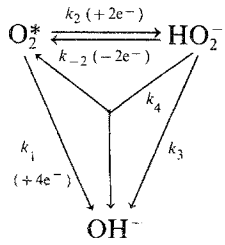

where (b), (i) and an asterisk indicate bulk, interface and adsorbed O_2 concentrations, respectively. The rate constants k_1, k_2 and k_{-2}, k_3 and k_4 relate to the four-electron direct reduction to OH^-, forward and backward rate constants for the two-electron process, the electrochemical reduction of HO_2^- to yield OH^- and the heterogeneous catalytic decomposition of HO_2^-, respectively.

Oxygen discharge at gold and silver during cyanidation falls in the range of two to four electrons per mol O_2. The kinetics of the cathodic O_2 discharge are best developed in terms of a mixed diffusion plus change transfer process incorporating the adsorption

of O_2. The general kinetic treatment is analogous to that presented for the anodic dissolution presented above. Equation 14 expresses the cathodic current density for the diffusion part of the reaction

$$i_c = -k'_d([O_2] - [O_2]_i) \quad (15)$$

The concentrations of dissolved oxygen in the bulk of solution and at the interface are represented by $[O_2]$ and $[O_2]_i$, respectively, and $k'_d = D_{O_2} z_c F/\delta$.

As before, the charge transfer component of the cathodic reaction is analysed in terms of the Butler–Volmer expression, neglecting back-reaction kinetics:

$$i_c = -k_c \theta_c \exp\left(\frac{-\alpha_c F E_c}{RT}\right) \quad (16)$$

where i_c is the cathodic current density, k_c is the rate constant for the charge transfer step; that is, containing either k_1 or k_2 as shown in Equation 14. Even though the overall mechanism for oxygen discharge may involve two or four electrons, Equation 16 based on a one-electron rate-determining step such as $O_2 + e^- = O_2^-$ (ads), as suggested by Zurilla *et al.* [14]. The term θ_c is the fraction of cathodic sites covered by adsorbed oxygen. For an ideal monolayer with single site occupied by O_2, the Langmuir adsorption isotherm applies, where θ_c is defined as

$$\theta_c = \frac{K[O_2]_i}{1 + K[O_2]_i} \quad (17)$$

Substituting the value of θ_c into Equation 16 yields

$$i_c = -\frac{k_c K[O_2]_i}{1 + K[O_2]_i} \exp\left(-\frac{\alpha_c F E_c}{RT}\right) \quad (18)$$

Now, by assuming steady-state conditions and small values for $[O_2]_i$, Equations 15 and 18 may be combined to give the following expression for $[O_2]_i$:

$$[O_2]_i = -\frac{k'_d[O_2]}{k_c K \exp(-\alpha_c F E_c/RT)} \quad (19)$$

This value for $[O_2]_i$ can now be substituted into Equation 18 to obtain an expression for the cathodic current:

$$i_c = -\frac{k'_d[O_2]}{1 + (k'_d/k_c)[O_2] \exp(\alpha_c F E_c/RT)} \quad (20)$$

It is important to recognize that this expression yields a diffusion-limiting current density as sufficiently negative potentials. However, as the electrodes potential increases (that is, low cathodic potentials), the right-hand part of the denominator becomes significantly greater than unity and Equation 20 reduces to

$$i_c = -k_c \exp\left(\frac{-\alpha_c F E_c}{RT}\right) \quad (21)$$

It should be recognized that Equation 21 is equivalent to Equation 16 for the special case when $\theta_c = 1$. This is reasonable since, at low cathodic potential, the rate of oxygen discharge is lower than the rate of diffusion and there is an accumulation of oxygen at the surface. The cathodic current density in this potential region is clearly independent of $[O_2]$. Inspection of the data of Kudryk and Kellogg [8] show this to be the case for reduction of oxygen at a gold cathode. At potentials between 0.05 and 0.15 V (versus standard hydrogen electrode (SHE)), the cathodic current was essentially independent of oxygen concentration between 21 and 99.5% O_2.

3. Experimental details

Electrochemical experiments were carried out at room temperature (23° C) in a 0.5 litre cell, using a Ag rotating-disc working electrode with a geometrical area of approximately 0.44 cm^2. Two graphite rods were used as counter-electrodes. Before each testing the working electrode was polished on 600-grit SiC paper and rinsed with distilled deionized water. Solutions were prepared by using sodium cyanide to adjust the cyanide content and sodium hydroxide to adjust the pH. The ionic strength was adjusted to 0.6 M using sodium sulphate.

A PAR Model 273 potentiostat was used to control the tests and current–potential curves were recorded using a Houston Instrument Model 200 *X–Y* recorder. All potential scans were started at the corresponding rest potential. Potentials were measured against a saturated calomel reference electrode (SCE) the potential of which was taken as 0.245 V on the SHE scale. All potential values in this paper are reported with respect to the SHE.

The anodic dissolution of silver in oxygen-free solutions containing known amounts of sodium cyanide was studied using a scan rate of 1 mV s^{-1}. Solutions containing 10^{-3} to 3×10^{-2} M cyanide at their natural pH values (pH 10.2–10.9) were used. The oxygen reduction reaction was studied in cyanide-free solutions at pH 11.9. The oxygen content of the electrolyte was fixed by bubbling oxygen–nitrogen mixtures of known compositions (10.4% O_2, air, 49.6% O_2, 68.2% O_2 and 99.9% O_2) for 20 min before each test.

4. Results and discussion

4.1. *Anodic oxidation of silver*

The anodic current density–potential curves shown in Fig. 2 are typical of the electrochemical behaviour of Ag in alkaline cyanide solutions. These data were obtained using a rotating disc speed of 500 rpm. Another series was carried out as a function of cyanide concentration using 700 rpm. At sufficiently high anodic potentials, Equation 8 reduces to the form

$$i_{a,l} = k_d [CN] \quad (22)$$

where $i_{a,l}$ is the limiting anodic current density. In Fig. 2 this is shown by the characteristic plateaux in the polarization curves. The current density becomes entirely diffusion controlled in this region and is directly proportional to the cyanide concentration. A plot of $i_{a,l}$ versus [CN] is shown in Fig. 3 for 500 and 700 rpm. These data provide excellent confirmation of

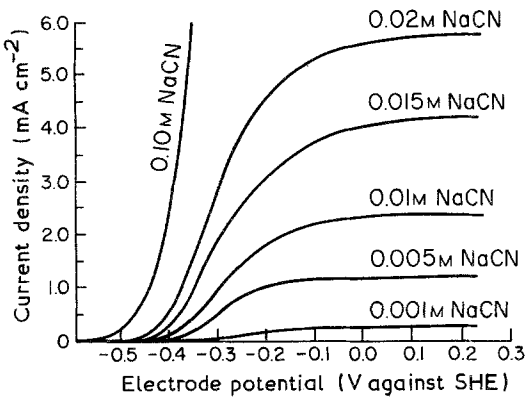

Fig. 2. Anodic oxidation of silver as a function of NaCN concentration using a rotating disc at 500 rpm.

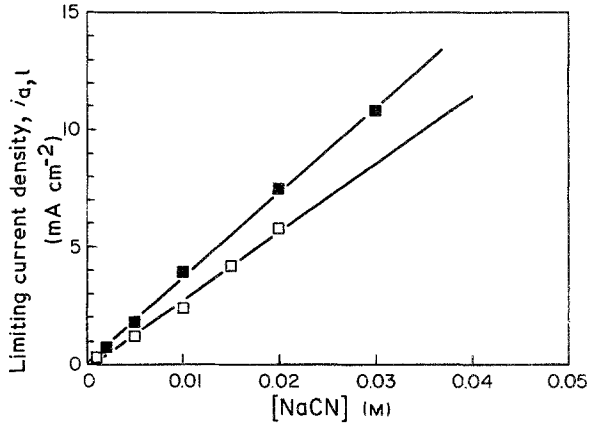

Fig. 3. Plot of limiting anodic currents as a function of NaCN concentration for (□) and (■) 700 rpm.

Equation 20 and also show that the current density (that is, the rate) in this region follows a first-order dependence with respect to the cyanide concentration. From the slopes of the lines in Fig. 3, k_d values of 289 and 364 mA l cm^{-2} mol^{-1} were obtained for 500 and 700 rpm, respectively.

Once the value of k_a, the charge transfer rate constant, is determined, Equation 8 can be used to predict the i–E behaviour for the anodic dissolution of Ag. To determine k_a, Equation 8 is inverted to yield

$$\frac{1}{i_a} = \frac{1}{k_d[\mathrm{CN}]} + \frac{1}{k_a[\mathrm{CN}]} \exp\left(\frac{-FE_a}{2RT}\right) \quad (23)$$

In this expression a value of 0.5 has been used for α_a. A plot of $1/i_a$ against exp $(-FE_a/2RT)$ should yield a straight line with a slope of $1/k_a$ [CN] and an intercept of $1/k_d$ [CN]. A test of Equation 23 is demonstrated in Fig. 4 for the mixed kinetic region for different values of [CN]. The values of k_a determined by this technique for silver are shown in Table 2, together with those of gold obtained from the analysis of the data of Kudryk and Kellogg [8].

Verification of the anodic dissolution model for various cyanide concentrations is shown in Fig. 5. The experimental curves were obtained using a disc rotation of 700 rpm. The full curves were calculated using the model and general values for k_a and k_d obtained from an analysis of electrochemical data for 700 rpm. The generalized rate expression, Equation 8, provides an excellent model for the anodic dissolution of silver and alkaline cyanide solutions.

4.2. *Cathodic reduction of oxygen on silver*

The cathodic reduction of oxygen at the silver electrode under alkaline conditions is shown in Fig. 6 for various partial pressures of oxygen. These curves show the general trend of approaching a characteristic diffusion-limited region. However, they do not exhibit well-defined plateaux as observed for the reduction of oxygen on gold. Recently, Adanuvor and White [19] found the cathodic reduction of oxygen on silver at high concentrations of NaOH to be a complex process lacking well-defined limiting currents.

The general shape of the polarization curves presented in Fig. 6 is also flatter than that observed for the discharge of oxygen on gold. Analysis of the experimental data shows that the cathodic current density fits

$$i_c = -\frac{k'_d\,[\mathrm{O_2}]}{1 + (k'_d/k'_c)\exp\,(\alpha_c FE_c/RT)} \quad (24)$$

where the constant $k'_c = k_c K'$ (K' is the Freundlich

Table 2. Charge transfer rate constants for the anodic oxidation of gold and silver in alkaline cyanide solutions

*Silver**				*Gold†*	
500 rpm		*700 rpm*		*300 rpm*	
[*CN*] (*M*)	k_a	[*CN*] (*M*)	k_a	[*CN*] (*M*)	k_a
1.0×10^{-3}	2.63×10^4	2.0×10^{-3}	0.64×10^4	7.68×10^{-4}	1.74×10^4
5.0×10^{-3}	5.44×10^4	5.0×10^{-3}	2.16×10^4	1.54×10^{-3}	3.19×10^4
1.0×10^{-2}	4.67×10^4	1.0×10^{-2}	4.96×10^4	2.69×10^{-3}	7.03×10^4
1.5×10^{-2}	6.77×10^4	2.0×10^{-2}	4.00×10^4	3.84×10^{-3}	4.73×10^4
2.0×10^{-2}	8.08×10^4	3.0×10^{-2}	5.07×10^4	1.54×10^{-2}	4.61×10^4
1.0×10^{-1}	4.67×10^4			7.68×10^{-2}	7.51×10^4
Average	5.38×10^4	Average	3.37×10^4	Average	4.80×10^4

*Rotating disc.
†Rotating cylinder.
Units for k_a are (mA l cm^{-2} mol^{-1}).

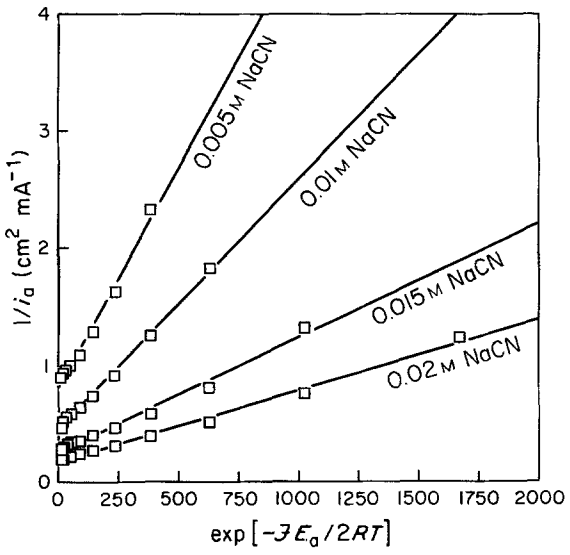

Fig. 4. Plot of $1/i_a$ against exp $(-FE_a/2RT)$ at various concentrations of NaCN, using a rotating disc at 500 rpm.

isotherm constant). This expression was derived assuming a one-electron rate determining step ($O_2 + e^- = O_2^-$(ads)) and a Freundlich adsorption model. The experimental results support the Freundlich-type isotherm for oxygen reduction on silver, since the current density is proportional to the oxygen concentration at all cathodic potentials as predicted by Equation 24. On the other hand, the Langmuir model best explains the reduction of oxygen on gold as predicted by Equation 20. Other adsorption models fail to fit the data adequately.

Based on these considerations, the expression for the cathodic current density for oxygen reduction on silver is

$$i_c = \frac{k_d' [O_2]}{1 + (k_d'/k_c') \exp(FE_c/4RT)} \qquad (25)$$

To be consistent with experimental values of current density the sign in Equation 25 is positive.

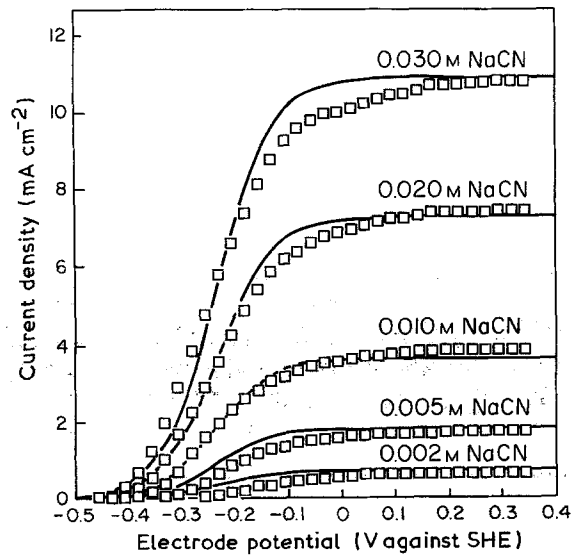

Fig. 5. Fit of mixed kinetic model to the anodic oxidation of silver for various concentrations of NaCN at 700 rpm, (□) experimental, (——) calculated.

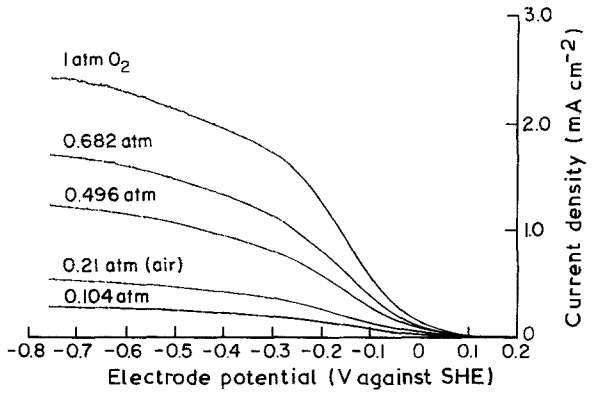

Fig. 6. Oxygen reduction on silver at pH 11.9 for various partial pressures of O_2 using a rotating disc at 500 rpm.

An apparent value of $\alpha_c = 0.25$ was used for the cathodic transfer coefficient in this expression. This value for α_c provides the best fit of the experimental results for the reduction of oxygen on silver.

At sufficiently negative cathodic potentials, Equation 25 reduces to the form

$$i_{c,l} = k_d' [O_2] \qquad (26)$$

where $i_{c,l}$ is the limiting current density for O_2 reduction. A plot of $i_{c,l}$ against $[O_2]$ is given in Fig. 7 for 500 and 700 rpm. From the slopes of these lines, k_d' values of 2.39 and 3.04 mA cm^{-2} atm^{-1} were obtained for 500 and 700 rpm, respectively. The same procedure outlined above to obtain the value of k_a for the anodic oxidation of silver was used to obtain the value of k_c for oxygen reduction on silver. A plot of $1/i_c$ against $\exp(FE_c/4RT)$ is shown in Fig. 8 for disc rotation of 500 rpm at different oxygen pressures. Excellent correlation is observed for the data in this region. Charge transfer rate constants are listed in Table 3.

Based on these values there appears to be a slight dependence of k_c' on the oxygen concentration, especially for the data obtained at 700 rpm. This in part reflects the complex nature of the oxygen discharge process. Complete analysis of the kinetics of oxygen reduction is beyond the scope of the present study. For the present treatment an average value of k_c' was determined and used in the calculation of the

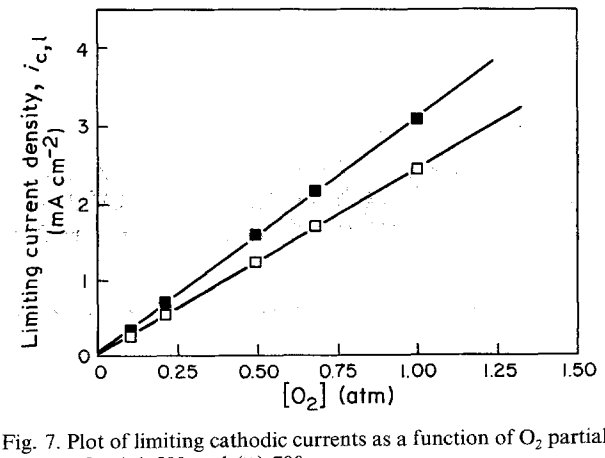

Fig. 7. Plot of limiting cathodic currents as a function of O_2 partial pressure for (■) 500 and (□) 700 rpm.

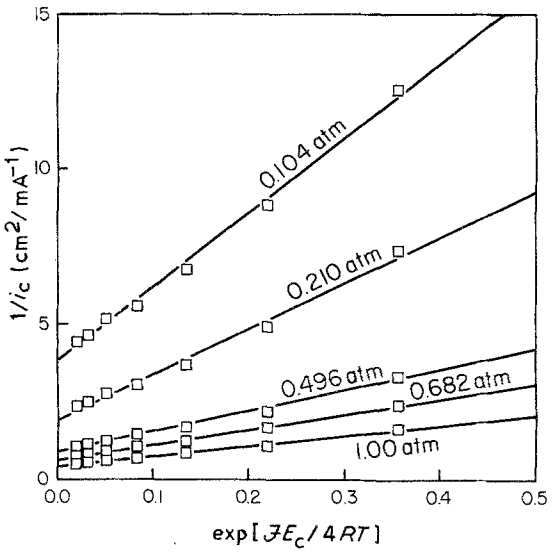

Fig. 8. Plot of $1/i_c$ against $\exp(FE_c/4RT)$ at various oxygen pressures using a rotating disc at 500 rpm.

cathodic response of oxygen or silver shown in Fig. 9. Based on the comparison in Fig. 9, the model for oxygen reduction on silver provides an excellent fit of the experiment results.

4.3. *Rotating-disc considerations*

A rotating-disc electrode was employed throughout this investigation. According to the basic theory of the rotating-disc electrode as published by Levich [26], the thickness of the diffusion boundary layer (δ) is given by

$$\delta = 1.61\left(\frac{D}{\nu}\right)^{1/3}\left(\frac{\nu}{\omega}\right)^{1/2} \qquad (27)$$

where D is the diffusion coefficient ($cm^2 s^{-1}$), ν is the kinematic viscosity ($cm^2 s^{-1}$) and ω is the angular speed of the rotating disc (s^{-1}).

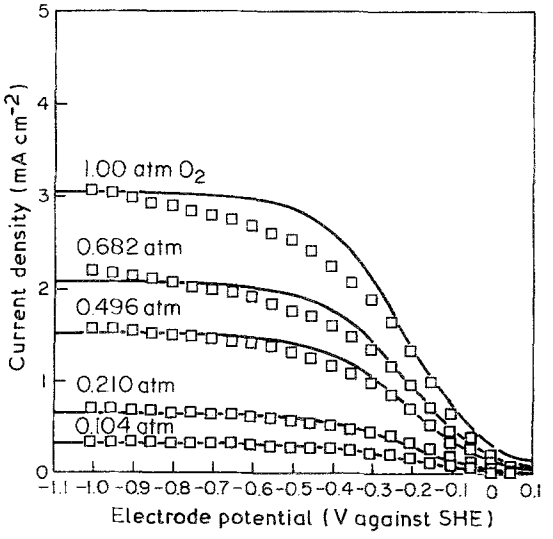

Fig. 9. Fit of mixed kinetic model to the cathodic reduction of oxygen on silver for various partial pressures of O_2, using a rotating disc at 700 rpm, (□) experimental, ——) calculated.

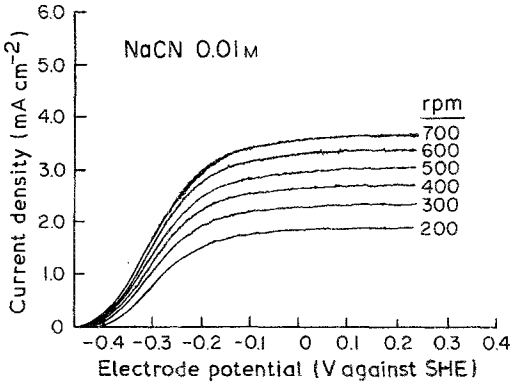

Fig. 10. Polarization data for the anodic oxidation of silver in 0.01 M NaCN at various disc rotation speeds.

A diffusion-controlled limiting current density is expressed as

$$i = \frac{zFDC}{1.61(D/\nu)^{1/3}(\nu/\omega)^{1/2}} \qquad (28)$$

or

$$i_{lim} = B\omega^{1/2} \qquad (29)$$

where $B = 0.62zFD^{2/3}\nu^{-1/6}C$ and C is the bulk concentration of the diffusing species.

Polarization curves for the anodic oxidation of silver in alkaline cyanide recorded at different rotation rates are shown in Fig. 10. Using the values of $i_{a,l}$ obtained from these curves, a plot of $i_{a,l}$ against $\omega^{1/2}$ is shown in Fig. 11. An excellent correlation exists for this data. From the slope of the line in Fig. 11 it is possible to calculate the experimental value of D_{CN}. The diffusion coefficient for cyanide under the conditions used in this investigation is $1.77 \times 10^{-5} cm^2 s^{-1}$. This value is extremely close to those reported elsewhere [27] for the sodium halides, assuming that the diffusion properties of cyanide are similar to those of the halides.

Oxygen reduction at the silver electrode was also examined as a function of the disc rotation speed. These results are presented in Fig. 12 for a constant partial pressure of oxygen of 0.682 atm. It is observed that the oxygen reduction current density is insensitive to the rotation speed at electrode potentials between −0.150 and 0.100 V (SHE). Similar behaviour was observed by Adanuvor and White [19] for the reduction of oxygen on silver and Enayetullah *et al.* [16] for oxygen reduction on platinum. The polarization curves

Table 3. Charge transfer rate constants for the cathodic reduction of oxygen at a silver electrode in alkaline solutions

$[O_2]$ (atm)	k'_c ($mA\,cm^{-2}\,atm^{-1}$)	
	500 r.p.m.	*700 r.p.m.*
0.104	0.40	0.54
0.210 (air)	0.33	0.46
0.496	0.31	0.33
0.682	0.30	0.34
1.000	0.30	0.32

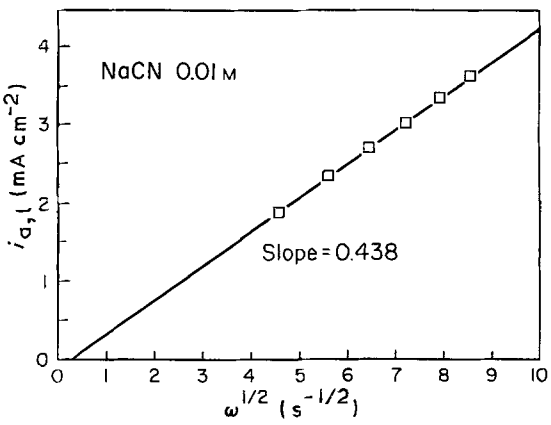

Fig. 11. Plot of limiting anodic currents as a function of $\omega^{1/2}$.

exhibit a relatively flat response in the mixed kinetic region and the absence of a distinct plateau representing the limiting current density attributed to O_2 reduction. The following approach will be used to analyse the cathodic reduction of oxygen in the mixed kinetic region. The following relationship can be derived by rearranging Equation 18:

$$\frac{1}{i_c} = \frac{1}{i_k} + \frac{1}{i_{c,l}} = \frac{1}{i_k} + \frac{1}{0.620 z_c F[O_2] D^{2/3} \nu^{-1/6} \omega^{1/2}} \quad (30)$$

where i_k represents the current in the absence of any diffusional effects (for example, at the foot of the wave of the irreversible charge transfer). A plot of $1/i_{c,l}$ against $1/\omega^{1/2}$ should be linear for a constant electrode potential. These plots are shown in Fig. 13 for different potentials. Lines of nearly the same slope are obtained. Based on this information a value for the diffusion coefficient of O_2 was calculated to be 1.60×10^{-5} cm^2 s^{-1}.

4.4 *Rate of cyanide dissolution*

As discussed by Wadsworth [10] the rate of cyanide leaching of gold and silver may be determined from the electrochemical data. The dissolution current (i_d) of the internally short-circuited cell is set by the conditions $E_a = E_c = E_m$ (mixed potential) and $i_a = i_c = i_d$. The value of i_d can be determined by

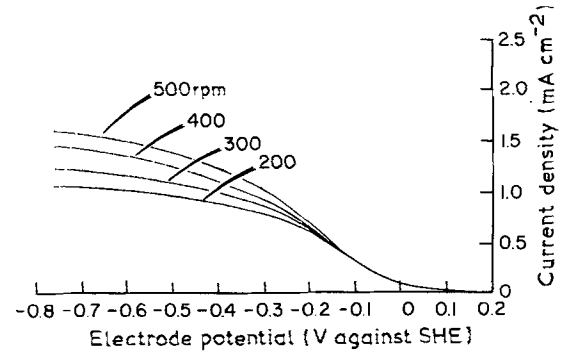

Fig. 12. Polarization data for the O_2 reduction on silver at various disc rotation speeds and 0.682 atm O_2.

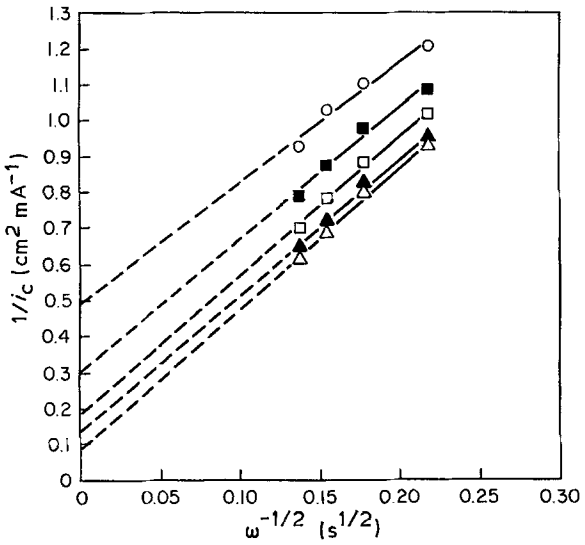

Fig. 13. Plot of $1/i_c$ against $\omega^{-1/2}$ at various potentials for the O_2 reduction on silver, (○) −0.31 V, (■) −0.41 V, (□) −0.51 V, (▲) −0.61 V, (△) −0.71 V.

combining Equations 8 and 20 for gold dissolution and Equations 8 and 24 silver dissolution.

It is convenient to compare the kinetic response of gold and silver by overlaying the anodic dissolution curves of gold and silver with the curves for the cathodic reduction of oxygen on gold and silver electrodes. The mixed kinetic model was used to calculate the respective polarization curves shown in Fig. 14. The broken curves represent the anodic oxidation of both gold and silver as a function of cyanide concentration between 10^{-3} and 10^{-1} M. As shown by this investigation, the anodic oxidation behaviour of gold and silver is for all practical purposes the same. The cathodic reduction of oxygen on gold and silver is plotted as the full curves for an oxygen partial pressure of 0.21 atm. In the mixed kinetic region the silver curve is noticeably lower than that of gold, mainly because of the apparent value of the cathodic transfer coefficient.

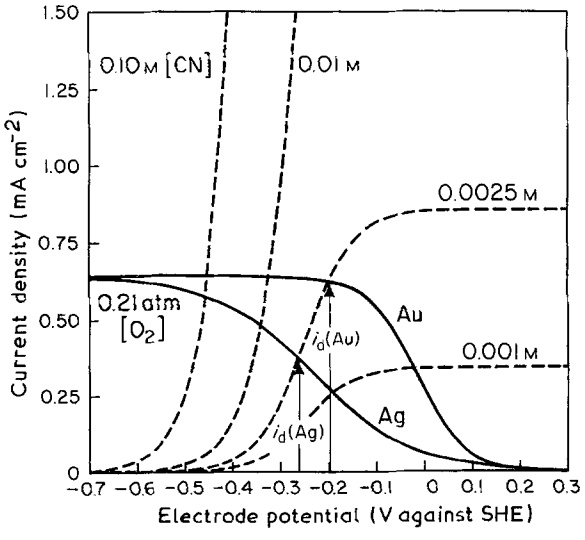

Fig. 14. Electrochemical data for the anodic oxidation of silver and gold and the cathodic reduction of O_2 on silver and gold calculated according to mixed kinetic models.

Intersection of the anodic and cathodic curves to the condition $E_a = E_c = E_m$ and $i_a = i_c = i_d$. It is readily apparent that at a cyanide concentration between 2.5×10^{-3} and 1×10^{-2} M (probably typical of most cyanidation operations) the value of $i_d(Ag) < i_d(Au)$. Under these conditions the rate of silver dissolution would be predicted to be lower than that of gold. Differences in the dissolution for the two metals become less significant for air when the cyanide concentration is at the extremes. Low concentrations of cyanide results in points of intersection on the plateau regions of the anodic curve where the rate is controlled by cyanide diffusion. At high cyanide concentrations the rate is controlled by oxygen diffusion.

5. Conclusions

The mechanism and rate-determining factors in the cyanidation of pure silver have been investigated. Experiments were performed on silver electrodes in an attempt to elucidate the fundamental differences between gold and silver cyanidation. The anodic oxidation of silver at various cyanide concentration follows a mixed kinetic model involving coupled mass transfer and charge transfer. A diffusion coefficient of 1.77×10^{-5} cm^2 sec^{-1} for cyanide was determined from the results of this investigation. Furthermore, the charge transfer rate constants for silver measured during this study and that of gold measured previously [8] are in favourable agreement. Based on these findings, the anodic oxidation of silver and gold in cyanide solutions exhibits essentially the same behaviour.

Oxygen reduction at the Ag surface was also studied. It was found that the oxygen reduction followed a kinetic model involving a mixed diffusion plus charge transfer process that incorporates the adsorption of O_2. As previously shown [12], the discharge of oxygen at a silver surface is markedly different from that at a gold surface. The basic differences are: (1) silver proceeds by a four-electron direct path instead of the two-electron path for gold; (2) oxygen adsorption appears to follow a Freundlich isotherm on silver and a Langmuir iostherm in gold; and (3) the transfer coefficient for oxygen reduction on silver is 0.25 whereas on gold it is 0.50. According to the difference in oxygen reduction on silver and gold, it is possible to prove that under typical cyanidation conditions silver dissolves at a rate slower than gold.

References

[1] J. S. MacArthur, R. W. Forrest and W. Forrest, British Patent 14 174 (1887).
[2] *Idem*, US Patents 403 202 and 418 137 (1989).
[3] G. Barsky, S. J. Swainson and N. Hedley, *Trans. AIME* **112** (1934) 660.
[4] E. Beyers, *J. Chem. Met. Soc., S. Afr.* **37** (1936) 37.
[5] I. A. Kakovskii and Y. B. Kholmanskikh, *Izv. Akad. Nauk SSSR, Otdel. Tekh. Nauk. Met. Toplivo*, No. 5 (1959) 97.
[6] *Idem, ibid.* No. 5 (1960) 207.
[7] G. A. Deitz and J. Halpern, *Trans. AIME* **197** (1953) 1109.
[8] V. Kudryk and H. H. Kellogg, *J. Metals* **6** (1954) 541.
[9] A. G. Sharpe, 'The Chemistry of Cyano Complexes of the Transition Metals', Academic Press, London (1976).
[10] M. E. Wadsworth, *Mining Engng* **37** (1985) 557.
[11] D. W. Kirk and F. R. Foulkes, *J. Electrochem. Soc.* **127** (1980) 1993.
[12] C. J. Van Velzen, A. G. Remijnse, G. J. Brug, M. Sluyters-Rehbach and J. H. Sluyters, *J. Electroanal. Chem.* **134** (1982) 87.
[13] P. Fisher and J. Heitbaum, *J. Electroanal. Chem.*, **112** (1980) 231.
[14] R. W. Zurilla, R. K. Sen and E. Yeager, *J. Electrochem. Soc.* **125** (1978) 1103.
[15] D. H. Evans and J. J. Lingane, *J. Electroanal. Chem.* **6** (1963) 283.
[16] M. A. Enayetullah, E. J. M. O'Sullivan and E. B. Yeager, *J. Appl. Electrochem.* **18** (1988) 763.
[17] K. Juttner, *Electrochim. Acta* **29** (1984) 1597.
[18] D. A. J. Rand and R. Woods, *J. Electroanal. Chem.* **31** (1971) 29.
[19] P. K. Adanuvor and R. E. White, *J. Electrochem. Soc.* **135** (1988) 2509.
[20] H. S. Wroblowa, Y. C. Pan and G. Razumney, *J. Electroanal. Chem.* **69** (1976) 195.
[21] M. Brezina, J. Koryta and M. Musilova, *Coll. Czech. Chem. Commun.* **33** (1968) 1026.
[22] N. A. Anastasijevic, S. Strubac and R. R. Adzic, *J. Electroanal. Chem.* **240** (1988) 239.
[23] A. Zwetanova and K. Juttner, *ibid.* **119** (1981) 149.
[24] E. Yeager, 'Electrocatalysis on Non-metallic Surfaces', *NBS Spec. Publ.* **445** (1976) 203.
[25] C. G. Fink and G. L. Putnam, *Trans. AIME* **187** (1950) 952.
[26] V. G. Levich, 'Physicochemical Hydrodynamics', Prentice-Hall, Englewood Cliffs, New Jersey (1962).
[27] T. W. Chapman, PhD Thesis, University of California–Berkeley, (1967).
[28] J. B. Hiskey, in 'Au and Ag Heap and Dump Leaching Practice' (edited by J. B. Hiskey), Society of Mining Engineers, New Jersey (1984) Ch. 1.